2017 IEEE/RSJ International Conference on Intelligent Robots and Systems (IROS)
September 24–28, 2017, Vancouver, BC, Canada

Design of a Soft Catheter for Low-Force and Constrained Surgery

Patrick Slade, Alex Gruebele, Zachary Hammond, Michael Raitor, Allison M. Okamura, and Elliot W. Hawkes

Abstract— **Surgeries involving interaction with soft tissue like the brain need to minimize shear and normal forces that can cause tissue damage or hemorrhage. Other surgeries require the ability to follow a complex, curved path, such as through an intestine or to a kidney stone. This paper presents a soft catheter that has the potential to aid in these challenging cases. The soft catheter is capable of apical extension in which the tip extends while the rest of the catheter remains stationary. This limits shear forces with the environment, easing movement of a body's tip through a constrained space. The soft catheter is pre-formed to patient-specific trajectories, meaning that normal forces against tissue would only arise due to errors between the actual and desired paths; we show decrease in normal force applied to the environment on the order of 100 compared to a standard catheter in a 30 degree bend. Setting the internal pressure allows for control of catheter stiffness, with a 500 times difference over the range of tested pressures. Manual operation to reach a surgical site requires only holding the correct orientation at the entry point into the body and setting the internal pressure of the catheter. This soft catheter could offer two benefits: the ability to apply low tissue interaction forces and reach challenging locations within the body.**

I. Introduction

A. Background

When performing minimally invasive operations, surgeons use endoscopes and catheters to visualize and deliver tools to a surgical site. Since these tools tend to be semi-rigid, it is difficult to navigate them through complex paths. Further, as they slide inside the body, they generate large shear forces, and as they pass through large bend angles along the path, they generate undesired normal forces. These challenges limit the types of operations performed by these tools.

We aim to develop soft catheters appropriate for difficult applications such as treatment of hydrocephalus in the brain. Hydrocephalus is a condition of abnormal accumulation of cerebrospinal fluid (CSF) in the brain ventricles that can lead to permanent brain damage or death if left untreated. It is estimated that 700,000 adults and 1 in 2000 infants in the United States suffer from idiopathic normal pressure hydrocephalus [1, 2]. The two treatments currently available to patients are CSF shunts and Endoscopic Third Ventriculostomy (ETV). ETV drains excess CSF by puncturing a hole in the floor of the third ventricle. It is often the primary treatment for hydrocephalus because it does not require implantation of a foreign body, and thereby avoids many of the long term complications associated with CSF shunts such as infection and device malfunction [3, 4, 5]. Currently ETV cannot be performed in all groups of patients because there is no safe straight path for the surgeon to access the ventricles without high risk of damage to brain tissue or hemorrhage [6]. One danger of performing ETV is possible physician error in guiding the endoscope. Errors in ETV occur more frequently in the physicians early career and often stem from applying excessive normal force when sliding a flexible endoscope through the passage of the ventricle [7].

In less sensitive parts of the body, increased access into constrained environments can enable interventions beyond the current limits of controllable endoscopes and catheters. Stones lodged in the calyces of the kidney are difficult to treat as standard catheters are unable to reach them. This leaves either percutaneous nephrolithotomy (passing a needle into the pelvic region) or laparoscopic procedures [8]. Conventional endoscopes are also unable to access the small intestine due to discomfort and lack of flexibility [9]. This presents a challenge for simple tasks such as imaging or collecting tissue samples without performing surgery.

These are only a few examples of the challenging surgeries that could potentially benefit from low contact forces and the ability to access constrained regions of the body.

B. Related Work

The use of catheters and endoscopes reduces patient trauma compared with open surgery techniques. Rigid endoscopes provide superior vision but are limited to reaching

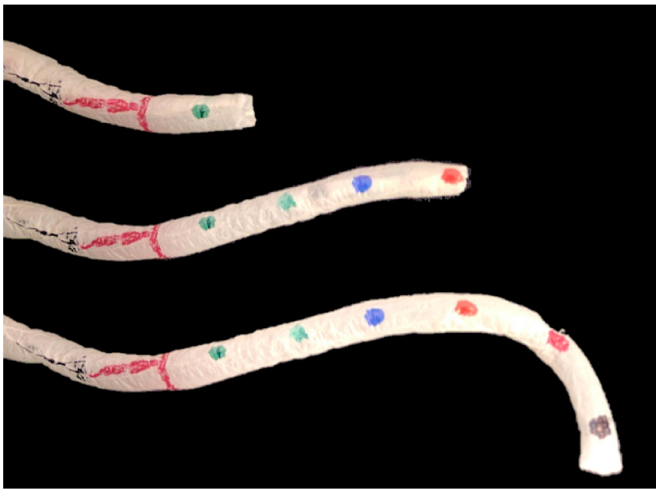

Fig. 1: Three stages during apical extension of the soft catheter following the trajectory for a brain ventricle.

This work is supported by the National Science Foundation Grant 1196335-1-QACCW and Graduate Research Fellowship Program under Grant DGE-1656518 and the Stanford Graduate Fellowship. The authors are with the Department of Mechanical Engineering at Stanford University, Stanford, CA 94305 USA. E.W.H. is also with the Department of Mechanical Engineering at University of California, Santa Barbara, CA 93106 USA. (e-mail: patslade@stanford.edu).

targets lying directly in line with the entry point [10]. Flexible endoscopes and fiberscopes allow a surgeon to reach targets off of a straight line, allowing the use of natural cavities. This minimizes trauma to soft tissue. Steering inside the body is enabled by active and passive deflection of the distal end of the scope, however, serious injury can occur when the endoscope does not bend fully to the intended trajectory [11]. Typical ventriculoscopes used in neuroendoscopic procedures have an active tip deflection of 160 degrees down and 100 degrees up [10]. Endoscopes for ureteroscopy, the diagnosis and treatment of intrarenal kidney stones, can reach tip deflections up to 270 degrees. This flexibility is often used when nearby the target to aid with visualization. However, in both cases, the deflection is greatly reduced by introducing a tool in the working channel [12].

The development of concentric-tube robots aims to tackle difficulty in steering catheters along an arbitrary 3-D trajectory through tissue while avoiding bone and organs. These robots actuate multiple tubes of varying stiffnesses that have a common axis, forming a mutually resultant curvature [13, 14]. The dexterity in these systems is important in tackling the challenges when removing large kidney stones. The maneuverability is limited by the number and stiffness of the concentric tubes, requiring careful design.

Capsule endoscopy is another strategy for following complex paths such as the small intestine [9]. These small devices are swallowed and enable visualization of the entire gastrointestinal tract as they pass through the body. This free-floating method limits the ability to control orientation which adds difficulty to view a specific target. Even in controllable capsule endoscopes there are challenges in performing safe operations such as taking a tissue sample [2, 15].

Finally, a hand-held controllable colonoscope can be driven through the colon, aided by an inverted sheath [16]. A set of wheels drive the inverted section of the sheath, everting it at the tip. The everting sheath eliminates shear friction between the scope and colon wall. The scope has a fixed length that moves from outside of the colon to inside as the sheath inverts. This process can be reversed. The forces from interacting with the colon wall steer it along the intestine.

In this paper we present the design of a novel soft catheter that employs a fundamentally different solution by increasing length from the tip as shown in Fig. 1 [17]. This strategy has advantages over traditional catheters because it does not impart forces on the body to shape or guide the catheter. The results suggest a reduction in shear and normal forces with peak reduction in the normal direction over 100 times. Experimental verification and modeling is done to show the ability to predict forces during insertion into the body. While these results are preliminary and are tested in artificial tissue with prototype catheters, they suggest the potential for impact in the area of minimally invasive medical procedures.

II. Design

A. Extension Method

The soft catheter consists of a thin-walled, hollow plastic tube that can be folded inside of itself, or inverted. This

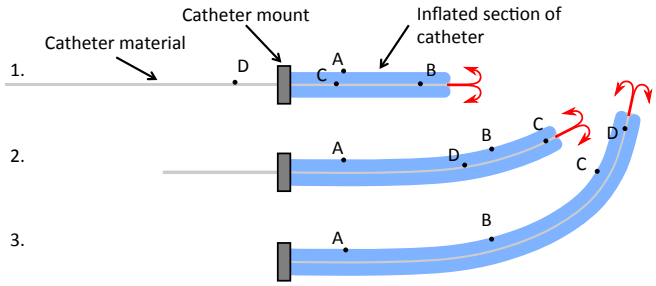

Fig. 2: Apical extension without sliding relative to the environment. Red arrows indicate motion of catheter material as it emerges and everts at the tip.

folding process is accomplished by tucking one end inside the tube using a rigid ramrod or by pulling a string secured to the end. Applied internal pressure causes the tucked material to extend out of the tip, or evert. It is able to minimize forces and follow trajectories due to the apical extension shown in three stages in Fig. 1. Once visible on the outside of the soft catheter, the colored dots do not move while the rest of the catheter finishes following the trajectory. Fig. 2 highlights this method of reaching a target surgical location, mapping the internal movement of material to stationary outer points along the trajectory. This pressure-driven tip extension is inspired by the principle of growth found in some plant and fungal cells [18, 19]. Once the catheter is fully extended, the internal pressure is increased to raise stiffness and minimize forces that tools apply to the tissue as they are passed to the surgical site. After the operation is complete, the internal pressure is released so the catheter completely deflates, minimizing stiffness, before being retracted manually. Currently, the pressure range tested for successful extension and tool passing is 15.5 kPa to 31.0 kPa. This ability to control stiffness is also shown with the fluidic actuation and granular jamming of a surgical manipulator[20]. In contrast, our soft catheter extends along a predefined trajectory, but is still capable of varying stiffness by changing internal pressure.

This movement strategy is also related to whole skin locomotion robots, which are comprised of a thin membrane formed into an elongated toroid, which are inspired by cytoplasmic streaming in ameobae [21, 22]. The skin of these robots is everted in a single continuous motion, similar to a tank tread. This type of robot requires shear force on the environment in order to locomote.

For a thin-walled vessel with internal pressure P, diameter D, and thickness t, the hoop stress is given by (1), and the longitudinal stress (approximate, assuming $t \ll D$) is given by (2). This indicates that the likely failure mode for the soft catheter due to internal pressure would be circumferential rupture. To account for this, future iterations of the soft catheter could include circumferential reinforcement in the form of strong and stiff fibers. Such reinforcement is already used in modern balloon catheters used for treating occlusions.

$$\sigma_\theta = \frac{Pd}{2t} \tag{1}$$

Fig. 3: (a) A pre-formed soft catheter. (b) The 3D-printed mold used to pre-form catheters.

$$\sigma_z = \frac{Pd}{4t} \tag{2}$$

The soft catheter described was tested with air as the working fluid. However, in a clinical setting a tear could result in a release of air into the body, which could cause a dangerous gas embolism. The soft catheter would be functionally similar with a saline solution as the working fluid. In that case, pressure would be maintained by a stiff plunger. Actuating this plunger with a screw or worm gear would apply pressure to the incompressible fluid within the reinforced and stiff, with respect to expansion, soft catheter body. The added advantage of using an essentially inextensible soft catheter material and highly geared plunger is that, if failure in the catheter wall occurs, the sudden slight increase in volume would cause an immediate drop in pressure of the fluid. This would avoid damaging soft tissue, such as brain tissue, if a failure were to occur during the procedure. Therefore, in this configuration the only limit on safe operating pressure is that which causes the catheter to reach the hoop stress limit.

B. Fabrication

The soft catheter is a low-density polyethylene (LDPE) sheet, with a thickness on the order of 10 microns, rolled into a tube. The exact thickness used in this paper was given in the manufacturer specifications as 13 microns. The thinnest possible material is desired to have the smallest bending stiffness to minimize resistance to eversion, improving apical extension and the accuracy of pre-formed angles, with the constraint of holding the required pressure. Standard guiding catheters used for ETV or kidney stone removal have a maximum diameter of 4 mm (12 French), with smaller diameters desired. Soft catheters are formed to the specified diameter and varying lengths using a tabletop heat sealer.

In order to achieve a trajectory, the soft catheter must be able to accurately hold the shape of various angles and radii of curvature for those angles. To form the catheter to a desired angle and curvature, the 3-D printed core is sheathed in the LDPE tube. Heat is applied to all sides of the core and catheter by a ULINE H-915 heat gun kept at a distance of two centimeters for approximately half of a second. The application of heat relaxes internal stress in the plastic, and it re-forms to the shape of the core seen in Fig. 3. To minimize errors between desired and actual angle after forming, the soft catheter and core diameters must match closely so that the plastic is taught and without wrinkles or loose material.

The catheter would require a patient specific 3-D trajectory found through imaging to reach a surgical site. We used models to find a path to pre-form the catheter following the fabrication process previously described. Using this pre-defined trajectory eliminates the need for manual steering and minimizes normal forces that might occur due to tissue impact when extending in the body. Fig. 4 steps through the process of a soft catheter being extended along a trajectory. The orientation during insertion was controlled manually. Previous registration techniques such as in [23] can be employed to obtain accurate orientation before extension. This path was generated from a brain ventricle model on the NIH 3-D Print Exchange [24]. This path was 3-D printed as a core and used to form a catheter for insertion. The soft catheter extending along this trajectory is shown in free space in Fig. 1, the desired shape is held without any force from an environment.

III. Results

A. Pre-forming the Catheter Path

The ability of the catheter to hold different combinations of angles and curvatures is shown in Fig. 5. 30 degree increments were tested up to a 150 degree bend with three curvatures and three trials for each combination. Ideally the desired angle would match the actual angle. The higher angles showed hysteresis and a final angle less than desired. For ranges of bend angles up to 90 degrees, all curvatures were able to meet the desired angle within a standard deviation of one degree or less.

B. Cantilever Beam Deflection

An inflatable cantilever beam model is employed to make predictions of the normal force caused by the error in the pre-formed angles. In [25], the equations to calculate the deflection of a beam due to a known tip load are derived. Deflection values are found for various dimensionless loads calculated as:

$$F_d = \frac{Pl}{pR^3}, \tag{3}$$

where P is the tip load (N), l is the length of the beam (mm), R is the radius (mm), and p is the internal pressure (kPa). This dimensionless load value (F_d) allows the deflections at the tip due to bending and shear to be taken from precomputed curves in [25].

Tip deflection of fixed-base cantilevered catheters of 20 mm length and 2 mm radius were measured for transverse loads from 1 to 4 grams. The catheters were mounted horizontally and inflated before quasi-static loading. Three trials were recorded for each combination of angle, radius, and pressure. The comparison in Fig. 6 shows that increasing internal pressure increases stiffness of the cantilever beam.

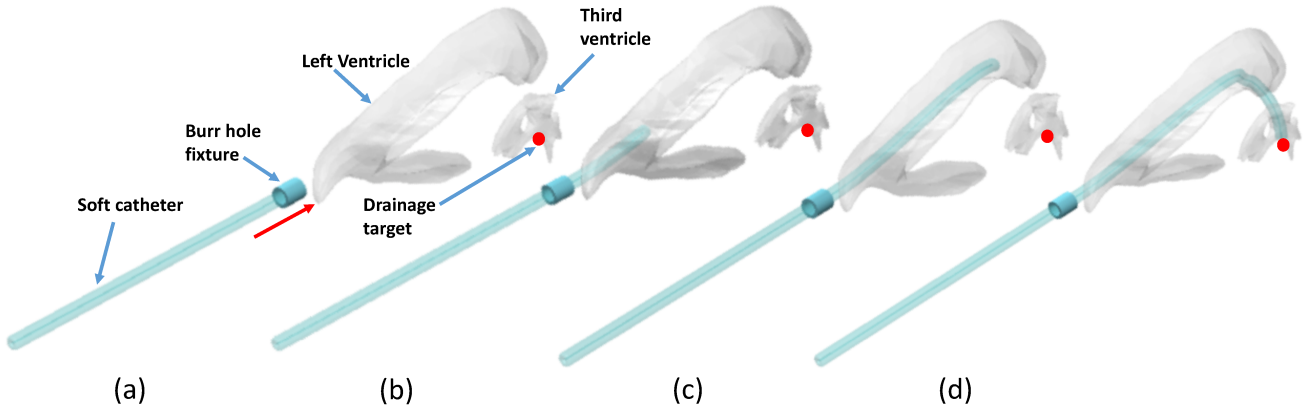

Fig. 4: Simulation of a soft catheter extending through a brain ventricles model: (a) prior to insertion into left ventricle, (b) partial growth, (c) approaching a sharp turn, (d) reaching a target.

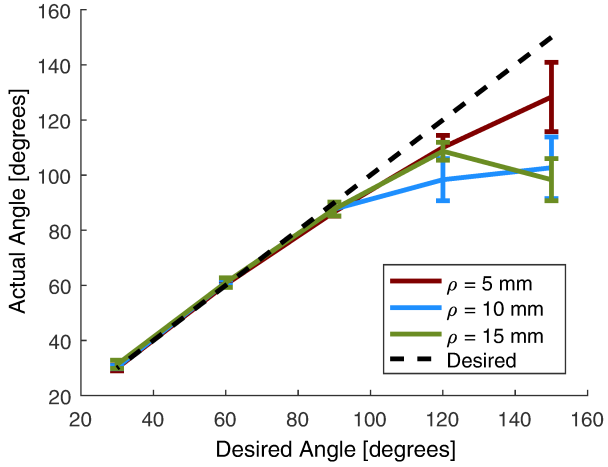

Fig. 5: Pre-formed bend angles at various radii of curvature and standard deviation bars.

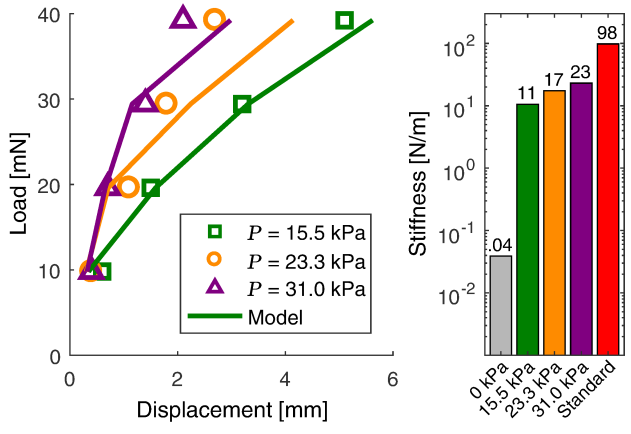

Fig. 6: *Left:* experimental and model displacements of a 20 mm cantilever with single point loads. *Right:* the stiffnesses of a soft catheter at various pressures and a standard catheter.

The precomputed curves used in [25] are most accurate for a ratio of length to radius of greater than 10. Shorter cantilever beam lengths were also tested but the percent differences between the model and experimental values for lengths 20 mm, 15 mm, and 10 mm were 22.1%, 66.5%, and 131.6%, respectively. Thus, only the deflection values for the length of 20 mm were used to predict forces due to significant pre-forming errors for other lengths.

Using the average force and deflection values in the cantilever beam tests with length of 20 mm and diameter 4 mm (12 French), an approximate linear stiffness was calculated for the soft catheter at each pressure. This same procedure was used to find the stiffness of a soft catheter with no internal pressure and a standard catheter for a length of 20 mm. Fig. 6 presents these values; the case of no internal pressure is on the order of 1000 times smaller than a standard catheter. Compared to the inflated soft catheter, there exists a roughly 500 times difference in stiffness. This ability to control stiffness presents advantages when trying to apply minimal forces while extending to the surgical site (low pressure), then increasing stiffness of a curved soft catheter to minimize the force that the straight tool applies to the tissue (high pressure), and finally adopting the lowest stiffness during retraction (no pressure).

C. Catheter and Surgical Wire Insertion

We evaluated the accuracy of our beam bending calculations in predicting normal forces due to errors in the pre-forming angle using a grounded ATI Nano17 force sensor with a rigidly mounted tube aligned to a second tube grounded at an angle shown in Fig. 7. The soft and standard catheters were extended through the curve and steady state forces of the catheters pushing on the tube were recorded. Data are shown in Fig. 8 for angles of 30 and 60 degrees with three trials for every measurement. The soft catheter forces were within the standard deviation bounds of what was predicted by the model. For angles less than 90 degrees this is within 0.57 degrees. The soft catheter in the 30 and 60

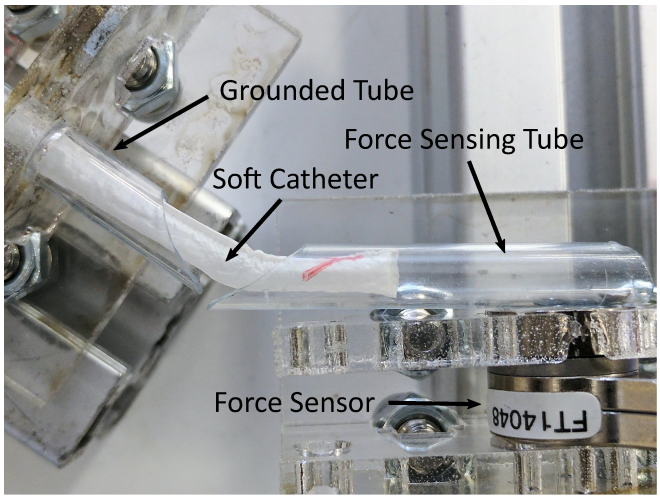

Fig. 7: Experimental setup used to measure normal forces during catheter extension and tool insertion.

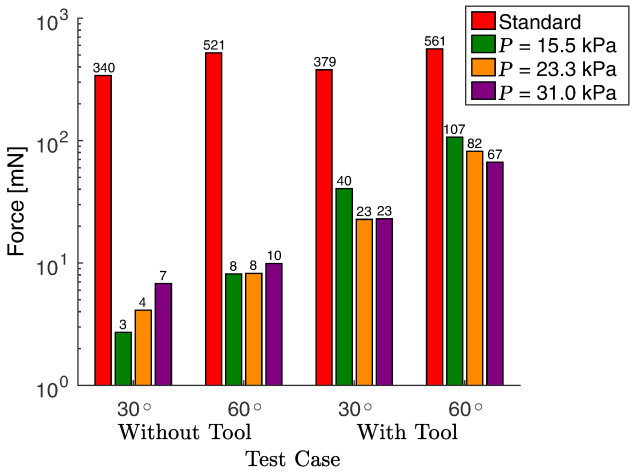

Fig. 8: Static forces applied by the catheters inserted in three trials with 30 and 60 degree bends. Tests were conducted with standard and soft catheters at various pressures.

degree bends applied 1.34% and 1.68% of the forces applied by the standard catheter.

Using the same experimental setup, a 1 mm (3 French) surgical wire was passed through the catheters. The total steady state force from the catheters and the wire is shown in Fig. 8. The small increase in tool force in the standard catheter shows that the initial large stiffness is changed relatively little, while the soft catheter varies significantly with pressure and angle. The average soft catheter force with the tool is 15.6% and 7.93% of the force applied by the standard catheter with the tool at 30 and 60 degrees. The stiffness of the surgical wire is relatively higher compared to the soft catheters, causing a larger change in applied forces than the standard catheter. Interestingly, larger pressures show smaller applied forces with the tool, because the higher pressure holds the curved shape better. This is in contrast to the no tool cases, when higher pressures show higher applied forces, due to the slight errors in the pre-formed shape.

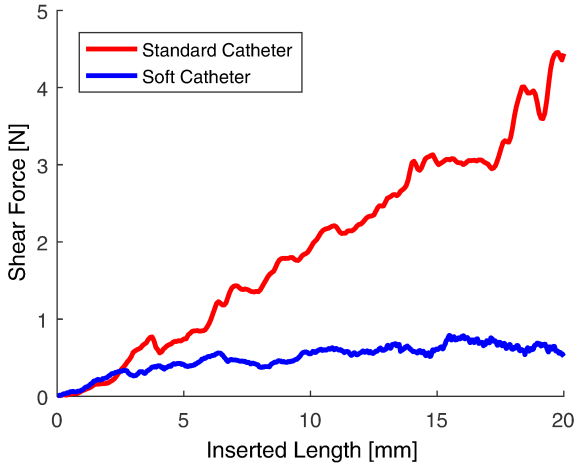

Fig. 9: Shear force applied by a standard catheter and the soft catheter inserted into our representative brain tissue.

D. Extension in Tissue Model

The interaction between the catheters and tissue was tested using a 19% bovine gelatin brain model, referred to as the phantom model. The gelatin concentrations were chosen to approximate the stiffness of human brain tissue based on previous work by [26]. The shear forces applied during apical extension of the soft catheter and insertion of a standard catheter were measured with a $2 \times 2 \times 2$ cm phantom cube mounted on an ATI Nano17 force sensor. Fig. 9 illustrates the linearly increasing shear force from the standard catheter. This indicates the surface area in contact with the phantom tissue and the corresponding surface area dependent shear force increases roughly linearly with insertion. The soft catheter has a small, non-zero and nearly constant shear force caused by the soft catheter pressing against the phantom tissue, but not from the sliding motion relative to the tissue.

Fig. 10 shows the $15 \times 9 \times 6$ cm phantom model with the same spline NIH brain ventricle trajectory shown in Figs. 1 and 4. This setup simulated a surgery in which the catheter is fed into the back of the head at a burr hole, and moved along the lateral ventricle into the third ventricle where a needle is used to puncture a hole. By puncturing the hole, excess CSF causing high pressure would be released, modeling a completed ETV. The low stiffness and high friction of the gelatin brain did not inhibit the soft catheter's ability to extend along the path as shown in Fig. 10 (a)-(c). A 3 French wire tool was fed along the catheter and out of its end, simulating the puncture to drain the CSF. The wire was then removed, and the pressure was decreased in order to soften the catheter fully before removing. The standard catheter, shown in Fig. 10 (d)-(f), was unable to navigate the trajectory and reach the surgical site as it punctured the phantom model at an approximately 90 degree bend. Standard catheters with a steerable tip or led by a guide wire would show improve performance and potentially reach the site, but their higher stiffness would apply larger normal forces and their method of moving through tissue would apply larger shear forces.

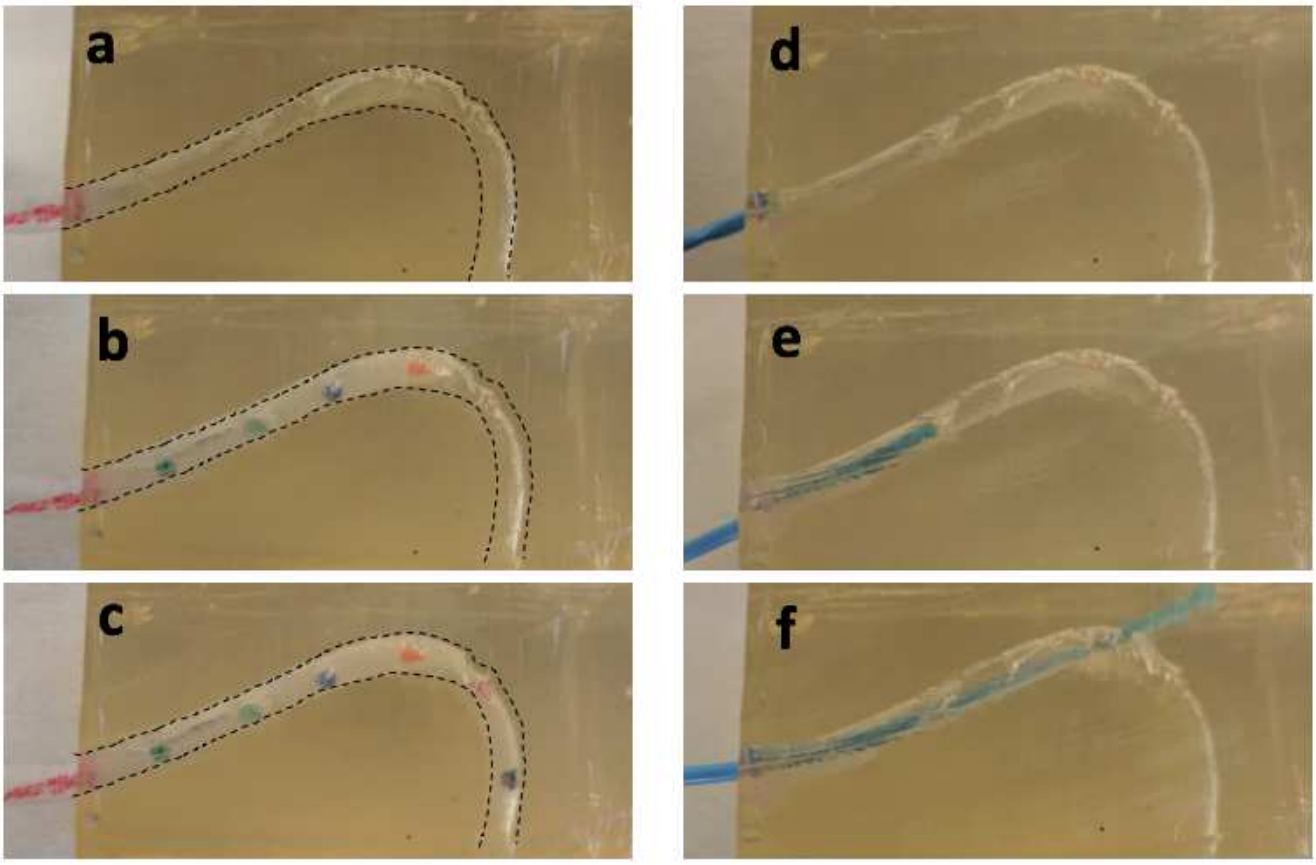

Fig. 10: Phantom brain tissue traversal from left ventricle entry to third ventricle drainage target. Soft catheter: (a) at entry point, (b) prior to 90 degree bend, (c) at drainage point. Standard catheter: (d) at entry point, (e) prior to 90 degree bend, (f) unsuccessful in achieving 90 degree bend.

IV. Discussion

A. Pre-forming the Catheter Path

The small standard deviation in pre-forming a bend angle of 90 degrees or less in the catheter allows for the prediction of normal forces along the trajectory. This allows for modification or selection of trajectories if the initial path results in forces that exceed the desired forces or the path is not the desired shape. Errors when pre-forming bend angles larger than 90 degrees are due to hysteresis in the forming process as well as deformation during removal of the solid core. Using a core with multiple parts or a material that can be easily dissolved would improve the precision.

Once extended, the soft catheter we propose can be thought of as a passive, continuous, variable stiffness version of patient specific concentric-tube robots [27]. It has uniform stiffness and the ability to pass a standard 3 French surgical wire, but does not currently allow for the change of a predefined path like is possible with concentric-tube robots.

B. Catheter and Surgical Wire Insertion

With the reported decrease in normal forces applied to phantom tissue, lower risk surgeries may be possible, by minimizing the damage to brain or soft tissue. This could expand the patient population that can benefit from surgeries like ETV and also might allow surgeons freedom to choose complex, but less invasive or sensitive paths to the surgical site. Even when a tool is passed through the soft catheter, the normal force is substantially lower than a standard catheter. Stiffer tools decrease this difference but could be mitigated by reinforcing soft catheters to get higher pressure.

Extending the soft catheter at lower pressures maintains the safe, low forces while reaching the surgical site. The internal pressure could then be increased to a level to minimize the forces applied by the tool during insertion. Finally, the pressure could be set to zero after tool retraction, and the soft catheter could be retracted with very little force. This ability to control the stiffness of the soft catheter by orders of magnitude is helpful in minimizing normal forces.

C. Extension in Tissue Model

The shear force threshold suggests that there is no motion of the catheter relative to the environment. This is an important distinction from standard catheters as it means the shear forces on the tissue could be much smaller and not increase with insertion length and that the surface characteristics do not affect the extension as it travels through the body.

The ability of the soft catheter to safely and easily follow the ventricle trajectory to perform the simulated ETV surgery highlights its advantages in terms of low forces and constrained environments. Reaching the surgical site is made considerably simpler than with a standard catheter, as the

surgeon will only be controlling the length of the catheter. This process requires no manual manipulation, decreasing user error and the training necessary to accomplish a surgery. Simplifying and enabling a lower-skill level to accomplish the surgery could reduce the cost of needing a more skilled professional and decrease time in the operating room.

V. Conclusions

In order to extend the reach of catheters and endoscopes, this work presents a new soft catheter design capable of accurately tracking any trajectory with angles 90 degrees or less and radii of curvature 5 mm or greater. By relying on apical extension, the soft catheter travels inside constrained environments with minimal shear force. The ability to predefine the path through heat treatment allows for complex trajectories. This possibility extends the range of catheters to reach locations such as the small intestines and the calyces of the kidney. The normal forces minimized by preforming can be predicted by cantilever beam-bending models and are experimentally verified, allowing for safe trajectory selection before surgery. The ability to use standard surgical tools while still applying 6.4 to 12.6 times less force than standard push-catheters for 60 and 30 degree bends enables safer operations that limit tissue damage or potential for complications such as hemorrhage. The controllable stiffness allows for minimizing forces while extending, when passing tools to a surgical site, and for manual retraction.

Building upon this initial device, an exploration of possible surgical uses and variety of tools capable of being used in conjunction with our catheter is needed to realize its potential. Other materials such as water-proofed high-strength fabrics should be explored to improve robustness and resistance to puncture. The ability to provide steering and real-time control would also enable more reliable movement rather than relying on imaging and a pre-formed trajectory. This could enable the catheter to perform corrections without relying on other surgical methods if complications arose requiring access to a different area than originally desired. Methods to regulate the extension rate should be tested to travel at a safe, controlled rate to the desired location.

VI. Acknowledgements

The authors thank Joseph Greer and Laura Blumenschein for their help in setting up the pressure regulation hardware and software as well as Zane Zook and Tenzin Moenbook for their assistance in data collection and figure preparation.

References

[1] G. Cinalli, "Alternatives to shunting," *Child's Nervous System*, vol. 15, no. 11-12, pp. 718–731, 1999.

[2] S. Yim and M. Sitti, "Design and rolling locomotion of a magnetically actuated soft capsule endoscope," *IEEE Transactions on Robotics*, vol. 28, no. 1, pp. 183–194, 2012.

[3] A. V. Kulkarni, J. M. Drake, C. L. Mallucci, S. Sgouros, J. Roth, S. Constantini, C. P. N. S. Group, *et al.*, "Endoscopic third ventriculostomy in the treatment of childhood hydrocephalus," *The Journal of Pediatrics*, vol. 155, no. 2, pp. 254–259, 2009.

[4] P. Kamalo, "Point of view: Exit ventriculoperitoneal shunt; enter endoscopic third ventriculostomy (etv): contemporary views on hydrocephalus and their implications on management," *Malawi Medical Journal*, vol. 25, no. 3, pp. 78–82, 2013.

[5] E. W. Sankey, C. R. Goodwin, I. Jusué-Torres, B. D. Elder, J. Hoffberger, J. Lu, A. M. Blitz, and D. Rigamonti, "Lower rates of symptom recurrence and surgical revision after primary compared with secondary endoscopic third ventriculostomy for obstructive hydrocephalus secondary to aqueductal stenosis in adults," *Journal of Neurosurgery*, vol. 124, no. 5, pp. 1413–1420, 2016.

[6] T. Charles, "Complications of endoscopic neurosurgery.," *Child's Nervous System*, vol. 12.5, pp. 248–253, 1996.

[7] S. P. Ambesh and R. Kumar, "Neuroendoscopic procedures: Anesthetic considerations for a growing trend: a review," *Journal of Neurosurgical Anesthesiology*, vol. 12, no. 3, pp. 262–270, 2000.

[8] E. M. Worcester and F. L. Coe, "Calcium kidney stones," *New England Journal of Medicine*, vol. 363, no. 10, pp. 954–963, 2010.

[9] G. Iddan, G. Meron, A. Glukhovsky, and P. Swain, "Wireless capsule endoscopy," *Nature*, vol. 405, no. 6785, p. 417, 2000.

[10] G. Cinalli, "Endoscopic third ventriculostomy," *Pediatric Hydrocephalus*, pp. 361–388, 2005.

[11] S. P. Ambesh and K. Raj, "Neuroendoscopic procedures: Anesthetic considerations for a growing trend," *Journal of Neurosurgical Anesthesiology*, vol. 12, no. 3, pp. 262–270, 2000.

[12] F. Pasqui, F. Dubosq, K. Tchala, M. Tligui, B. Gattegno, P. Thibault, and O. Traxer, "Impact on active scope deflection and irrigation flow of all endoscopic working tools during flexible ureteroscopy," *European Urology*, vol. 45, pp. 58–64, 2004.

[13] R. J. Webster, A. M. Okamura, and N. J. Cowan, "Toward active cannulas: Miniature snake-like surgical robots," in *IEEE/RSJ International Conference on Intelligent Robots and Systems*, pp. 2857–2863, 2006.

[14] P. Sears and P. Dupont, "A steerable needle technology using curved concentric tubes," in *IEEE/RSJ International Conference on Intelligent Robots and Systems*, pp. 2850–2856, 2006.

[15] H. Park, S. Park, E. Yoon, B. Kim, J. Park, and S. Park, "Paddling based microrobot for capsule endoscopes," in *IEEE International Conference on Robotics and Automation*, pp. 3377–3382, IEEE, 2007.

[16] T. Rösch, A. Adler, H. Pohl, E. Wettschureck, M. Koch, B. Wiedenmann, and N. Hoepffner, "A motor-driven single-use colonoscope controlled with a hand-held device: a feasibility study in volunteers," *Gastrointestinal endoscopy*, vol. 67, no. 7, pp. 1139–1146, 2008.

[17] E. W. Hawkes, L. H. Blumenschein, J. D. Greer, and A. M. Okamura, "A soft robot that navigates its environment through growth," Science Robotics, jul 2017.

[18] E. W. Dent and F. B. Gertler, "Cytoskeletal dynamics and transport in growth cone motility and axon guidance," *Neuron*, vol. 40, no. 2, pp. 209–227, 2003.

[19] R. R. Lew, "How does a hypha grow? The biophysics of pressurized growth in fungi," *Nature Reviews Microbiology*, vol. 9, no. 7, pp. 509–518, 2011.

[20] M. Cianchetti, T. Ranzani, G. Gerboni, I. De Falco, C. Laschi, and A. Menciassi, "STIFF-FLOP surgical manipulator: Mechanical design and experimental characterization of the single module," in *IEEE/RSJ International Conference on Intelligent Robots and Systems*, pp. 3576–3581, 2013.

[21] D. W. Hong, M. Ingram, and D. Lahr, "Whole skin locomotion inspired by amoeboid motility mechanisms," *Journal of Mechanisms and Robotics*, vol. 1, no. 1, p. 011015, 2009.

[22] J. C. McKenna, D. J. Anhalt, F. M. Bronson, H. B. Brown, M. Schwerin, E. Shammas, and H. Choset, "Toroidal skin drive for snake robot locomotion," in *IEEE International Conference on Robotics and Automation*, pp. 1150–1155, 2008.

[23] H. Zhong, T. Kanade, and D. Schwartzman, "virtual touch: An efficient registration method for catheter navigation in left atrium," *Medical Image Computing and Computer-Assisted Intervention*, pp. 437–444, 2006.

[24] "NIH 3D print exchange," *National Institutes of Health*.

[25] R. Comer and S. Levy, "Deflections of an inflated circular-cylindrical cantilever beam," *AIAA Journal*, vol. 1, no. 7, pp. 1652–1655, 1963.

[26] S. A. Kruse, G. H. Rose, K. J. Glaser, A. Manduca, J. P. Felmlee, C. R. Jack, and R. L. Ehman, "Magnetic resonance elastography of the brain," *Neuroimage*, vol. 39, no. 1, pp. 231–237, 2008.

[27] T. K. Morimoto, M. H. Hsieh, and A. M. Okamura, "Robot guided sheaths (RoGS) for percutaneous access to the pediatric kidney: Patient-specific design and preliminary results," in *ASME Dynamic Systems and Control Conference*, 2013.